High-resolution Laser Spectroscopy of NO2 just above the X2 A1-A2B conical intersection: Transitions of K_=1 stacks

Biesheuvel, C.A.; Bulthuis, J.; Janssen, M.H.M.; Stolte, S.; Snijders, J.G.

published in
Journal of Chemical Physics
2000

DOI (link to publisher)
10.1063/1.480936

document version
Publisher's PDF, also known as Version of record

High-resolution laser spectroscopy of NO_2 just above the $\tilde{X}^2A_1-\tilde{A}^2B_2$ conical intersection: Transitions of $K_-=1$ stacks

C. A. Biesheuvel,[a] J. Bulthuis, M. H. M. Janssen, and S. Stolte
Laser Centre and Department of Physical Chemistry, Faculty of Sciences, Vrije Universiteit, de Boelelaan 1083, 1081 HV Amsterdam, The Netherlands

J. G. Snijders
Theoretical Chemistry, Materials Science Centre, Rijksuniversiteit Groningen, Nijenborgh 4, 9747 AG Groningen, The Netherlands

(Received 30 March 1999; accepted 1 December 1999)

The complexity of the absorption spectrum of NO_2 can be attributed to a conical intersection of the potential energy surfaces of the two lowest electronic states, the electronic ground state of $^2A_1$ symmetry and the first electronically excited state of $^2B_2$ symmetry. In a previous paper we reported on the feasibility of using the hyperfine splittings, specifically the Fermi-contact interaction, to determine the electronic ground state character of the excited vibronic states in the region just above the conical intersection; 10 000 to 14 000 cm^{-1} above the electronic ground state. High-resolution spectra of a number of vibronic bands in this region were measured by exciting a supersonically cooled beam of NO_2 molecules with a narrow-band Ti:Sapphire ring laser. The energy absorbed by the molecules was detected by the use of a bolometer. In the region of interest, rovibronic interactions play no significant role, with the possible exception of the vibronic band at 12 658 cm^{-1}, so that the fine- and hyperfine structure of each rotational transition could be analyzed by using an effective Hamiltonian. In the previous paper we restricted ourselves to an analysis of transitions of the $K_-=0$ stack. In the present paper we extend the analysis to transitions of the $K_-=1$ stack, from which, in addition to hyperfine coupling constants, values of the A rotational constants of the excited NO_2 molecules can be determined. Those rotational constants also contain information about the electronic composition of the vibronic states, and, moreover, about the geometry of the NO_2 molecule in the excited state of interest. The results of our analyses are compared with those obtained by other authors. The conclusion arrived at in our previous paper that determining Fermi-constants is useful to help characterize the vibronic bands, is corroborated. In addition, the A rotational constants correspond to geometries that are consistent with the electronic composition of the relevant excited states as expected from the Fermi-constants. © *2000 American Institute of Physics.* [S0021-9606(00)01508-7]

I. INTRODUCTION

Although the nitrogen dioxide molecule is a simple near-prolate asymmetric rotor, its absorption spectrum is very dense and has a chaotic appearance (see, e.g., Refs. 1 and 2; recent absorption measurements over an extended frequency range are reported in Ref. 3). The high number of absorption lines is a result of the conical intersection of the electronic ground state of $^2A_1$ symmetry and the first electronically excited state of $^2B_2$ symmetry.[4] Above the conical intersection, which occurs around 10 000 cm^{-1},[5] the antisymmetric stretch couples the high b_2 vibrational levels of the electronic ground state and the low a_1 vibrational levels of the first electronically excited state to hybrid states with B_2 vibronic symmetry.[6,7]

To determine the contribution of both diabatic electronic states in the different hybrid states, we measure the hyperfine structure of the vibronic bands. The hyperfine structure is mainly caused by the Fermi-contact interaction. Considering the two electronic states involved, the Fermi-contact interaction constant in the electronic ground state is found to be 147.26 MHz,[8] whereas the Fermi-contact interaction term in the first electronically excited pure diabatic state will be almost zero.[9] So the magnitude of the Fermi-contact interaction term of the hybrid state provides information about the contribution of the high vibrational levels of the electronic ground state in the excited hybrid state.

In a previous paper we presented the results of the measurements of 16 vibronic bands of the $K_-=0$ stack in the energy range of 11 210–13 680 cm^{-1}.[10]

Only in a few cases have the transitions of the $K_-=1$ stack been assigned to a vibronic band.[11–14] This is not surprising since the identification of the various transitions is difficult. We successfully relied on those assignments to measure fully resolved hyperfine spectra of the 13 352 cm^{-1} vibronic band.[15] A transition of the $K_-=1$ stack can consist of more than two groups of lines, as is often observed for the $K_-=0$ stack, and can cover a rather large frequency range.[10,15] The transition frequency of a transition of the $K_-=1$ stack depends strongly on the value of the A' rotational constant, which can vary greatly going from one vibronic band to another. For instance, A_{A_1} for the (0,16,1)

[a]Present address: Department of Chemistry, University of Rochester, Rochester, New York 14627.

excited level at 13 316.7 cm^{-1} of the electronic ground state is calculated to be 16.84 cm^{-1},[11] in great contrast to $A_{B_2} = 2.84\ cm^{-1}$ calculated for the equilibrium geometry of the first electronically excited state.[16] So, it is not unlikely that different transitions of the $K_- = 1$ stack overlap and that an experimental spectrum therefore consists of groups of lines corresponding to transitions of different transitions of the $K_- = 1$ and $K_- = 0$ stack.

In this paper we present the measurements of the first systematic high-resolution study of NO_2 of the $K_- = 1$ stack of the vibronic bands at 13 395, 13 184 and 11 210 cm^{-1} using bolometric detection.[17] We will show that for the measured spectra of these vibronic bands the rovibronic interactions are weak enough not to perturb the regular rotational structure.

Of the vibronic band at 12 658 cm^{-1} we present the complex spectrum of the region where the R(1) $K_- = 1$ and R(0) $K_- = 0$ transitions overlap. To help assign the transitions in these overlapping spectra, the lower P- and R-transitions as well as the lowest R(0) transition of the lowest hot band of the $K_- = 0$ stack are presented.

Information about which vibrational levels of the electronic ground state contribute to the vibronic state is achieved by determining the A' rotational constant.

II. EXPERIMENT

The experiments are carried out using a homemade molecular beam machine. The apparatus will be described only briefly; for a more extensive description see Ref. 10.

The molecular beam machine consists of three chambers: a source chamber, an interaction chamber and a detector chamber.

The measurements are done with a 5% NO_2 beam seeded in helium and expanded through a 90 μm nozzle into the source chamber, leading to a rotational temperature of about 8 K. Before the beam reaches the bolometer detector it is collimated several times, resulting in a Doppler width of about 7 MHz.

In the interaction chamber a chopped laser beam crosses the molecular beam 29 times at almost right angles, leading to a Doppler shift to the blue of about 45 MHz.

The laser light has a bandwidth of less than 1 MHz and is created with a single mode continuous wave (cw) Ti:Sapphire laser pumped by an all-lines Ar^+-laser. The typical output power used to measure the spectra is about 0.5 W.

For the detection we use a composite silicon bolometer (Infrared Laboratories) at a working temperature of 1.6 K. The signals are measured phase-sensitively.

Simultaneously with the bolometer signal, frequency markers from a homemade temperature stabilized etalon (150 ± 0.2 MHz) are recorded for relative frequency assignment. The absolute frequencies are measured with a wavemeter (Burleigh) with an accuracy of 600 MHz according to the specifications of the manufacturer.

III. THEORY AND ANALYSIS

Considering NO_2 as a prolate top, the lowest rotational level $N'' = 1$ of the $K_- = 1$ stack of the electronic ground state is equal in energy to the $N'' = 4$ rotational level of the $K_- = 0$ stack. The population of the $N'' = 1$, $K_- = 1$ level is about two-thirds of the population of the $N'' = 0$, $K_- = 0$ level at a rotational temperature of 8 K estimated for our molecular beam. Taking into account the Hönl-London factors for a symmetric top molecule, the intensity of the R(1) $K_- = 1$ transition is expected to be about one-third the intensity of the R(0) $K_- = 0$ transition.

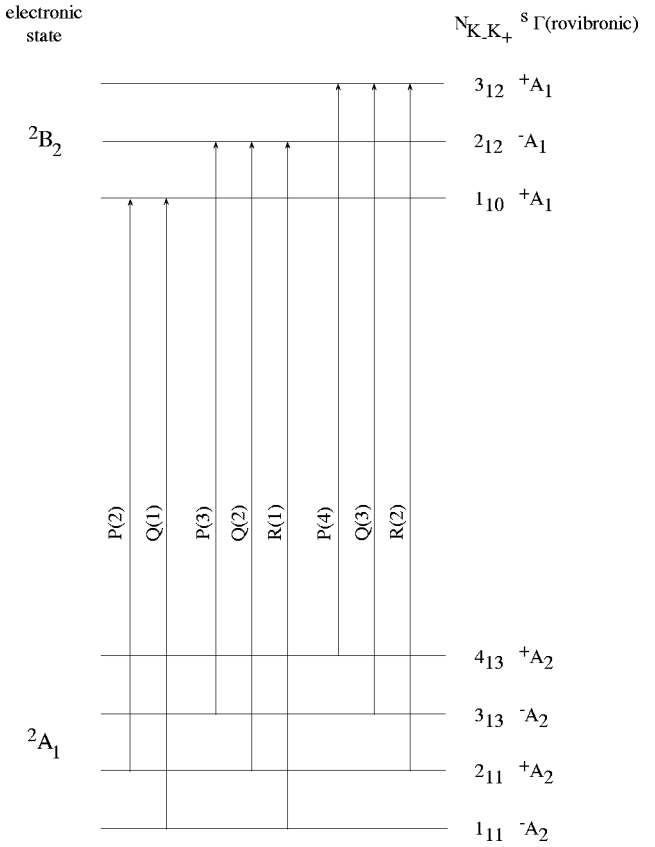

FIG. 1. Lowest rotational levels and corresponding transitions of the $K_- = 1$ stack ($v_3'' = v_3' = 0$). The fine- and hyperfine structure splittings are omitted for clarity.

The selection rules for the electric dipole transitions do not change going from the $K_- = 0$ stack to the $K_- \neq 0$ stacks, so $\Delta K_- = 0$ still holds, and only transitions between rotational levels of the electronic ground state and the first electronically excited state with A_1 and A_2 rovibronic symmetry are electric dipole allowed for $v_3' - v_3''$ even. For the bands discussed in this paper $v_3'' = 0$. Here, v_3' and v_3'' label the number of quanta in the asymmetric stretch vibration, which has b_2 symmetry, where the prime and double prime refer to the electronically excited state and the electronic ground state, respectively. The rotational levels of the $K_- = 0$ stack only exist for either even N (electronic ground state) or odd N (first electronically excited state), and thus can give rise to P- and R-branches only. $K_- \neq 0$ stacks comprise even as well as odd N rotational levels in the electronic ground state and first electronically excited state, and consequently the $K_- = 1$ stack has Q-branches in addition to P- and R-branches. Figure 1 is a schematic representation of the lowest rotational levels of the $K_- = 1$ stack and the most intense transitions starting from these levels. The corresponding represen-

tation of the hyperfine levels of the $K_- = 0$ stack is given in Fig. 2 of Ref. 10. The rotational levels are labeled as $N_{K_-K_+}$, in which K_- and K_+ are the projections of **N** on the symmetry axis in the prolate and oblate limit, respectively. The rovibronic symmetries are also indicated. For instance, the rovibronic symmetry of the $\tilde{A}\,^2B_2\,2_{12}\,v_3' = 0$ state is A_1. This follows, since for $N = 2$, $K_- = 1$, $K_+ = 2$, the rotational symmetry is B_2.[18] Furthermore, because the vibrational symmetry is a_1 $(v_3' = 0)$ and the electronic symmetry is B_2, the rovibronic symmetry is A_1. The sign of the combination of both prolate symmetric top wave functions in the Wang function is added as a superscript s in Fig. 1: + for the symmetric combination, − for the antisymmetric combination. Note that for each value of K_- only one value of s is allowed by the Pauli principle, applied to the bosonic oxygen nuclei.

The spectra are analyzed by varying the fine- and hyperfine structure parameters in the rotational Hamiltonian for the excited state so as to obtain the best fit of the experimental line positions, using the nonlinear least squares procedure[19] of Levenberg-Marquardt as described previously.[10]

The fine structure splitting is calculated by the expression given by Lin[20] [see also Eq. (4), Ref. 10]. In this expression the rovibronic interactions between rotational levels of different vibronic bands are considered to be small, so the fine structure splitting can be described by an effective Hamiltonian in which only vibronic interactions play a role. The hyperfine splitting is described by two terms: a relatively large Fermi-contact interaction term and a usually much smaller dipolar spin-spin interaction term. The hyperfine structure constants of the electronic ground state are well known from microwave experiments. In simulating the spectra, the three spin-rotation constants[21] as well as the Fermi-contact constant and the dipolar electron spin-nuclear spin interaction constants[8] for the electronic ground state are kept fixed.

In the calculations we have used the J-coupling scheme as a basis, i.e., **N** and **S** $(S = 1/2)$ are coupled to an intermediate angular momentum **J**, which is then coupled with the nitrogen spin **I** $(I = 1)$ to the total angular momentum **F**. F is a good quantum number but J is only approximately so. In the spectra we have analyzed, mixing between J-states is not so strong that J completely loses its meaning, and therefore it is still useful for labeling the spectral lines (see caption to Fig. 2).

The (hyper)fine structure for the $K_- = 0$ stack can be determined using three adjustable parameters, the fine structure constant $\overline{\epsilon}' = (\epsilon'_{bb} + \epsilon'_{cc})/2$ [see Eq. (5), Ref. 10], the Fermi-contact interaction constant σ' [see Eqs. (7) and (8), Ref. 10] and the dipole-dipole interaction constant λ' [see Eqs. (10) and (11), Ref. 10].

Even from the spectra of the $K_- = 1$ stack we are not able to determine all three fine stucture constants for the first electronically excited state. So we use the fine structure splitting as the fit parameter instead of the fine structure constant ϵ_{NK} [see Eq. (4), Ref. 10] in simulating the transitions of the $K_- = 1$ stack. The fine structure splitting is given as the energy difference between the two fine structure levels in the

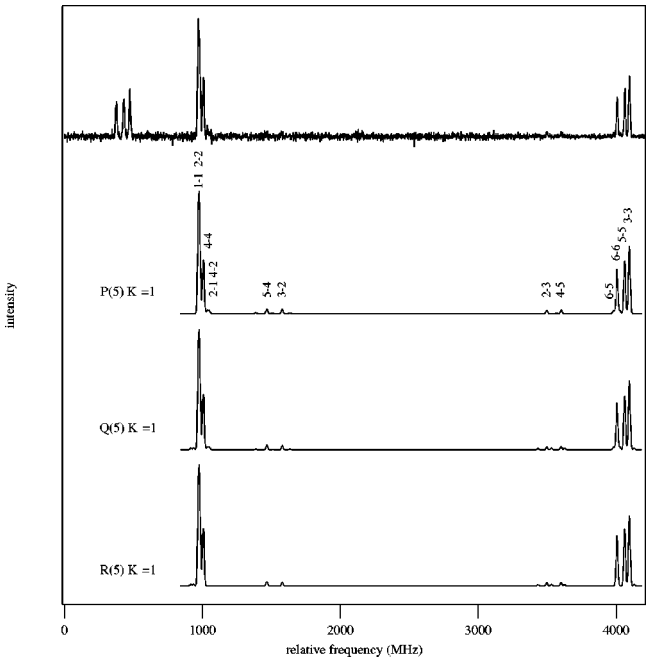

FIG. 2. A $K_- = 1$ transition of the 13 184 vibronic band at 13 184.85–13 185.00 cm^{-1}. Upper trace: experimental spectrum, lower traces: simulations of P- Q- and R-branch transitions, starting from $N'' = 5$. Transitions, except very weak ones, are labeled by $i - f$, where i and f are the energy level numbers of the ground state and the excited state, respectively. The energy levels belonging to rotational state N are numbered on the basis of the J-coupling scheme (see Sec. III) as follows. 1: $F = J + I$, $J = N + S$; 2: $F = J$, $J = N + S$; 3: $F = J + I$, $J = N - S$; 4: $F = J - I$, $J = N + S$; 5: $F = J$, $J = N - S$; 6: $F = J - I$, $J = N - S$, where $S = 1/2$ and $I = 1$. Note, however, that J is, in general, not a good quantum number.

J-coupling scheme limit ($J = N \pm 1/2$; for a positive splitting the $J = N + 1/2$ level is lowest in energy). For the hyperfine structure splitting of the excited state we use the Fermi-contact constant, σ', and the dipole-dipole constant, λ', as in the simulations of the spectra of the $K_- = 0$ stack. In fact, for $K_- \neq 0$ stacks the dipole-dipole tensor is described by two terms, λ and τ,[20] which, for a given K_- value, cannot be fitted independently. For convenience we have taken τ' equal zero, thus treating λ' as an effective parameter, which cannot be directly compared with λ' obtained for $K_- = 0$ stacks.

If the Fermi-contact interaction constant of the first electronically excited pure diabatic state is taken to be zero (spin-restricted one-determinant approximation), the value of the Fermi-contact interaction constant is a direct measure of the weight of the electronic ground state in the hybrid eigenstate (see also Ref. 10)

$$\langle \hat{\sigma} \rangle_n = q^n_{A_1}\, \sigma_{A_1}. \tag{1}$$

Here, $\langle \hat{\sigma} \rangle_n$ is the Fermi-contact constant for the hybrid vibronic state of interest, $q^n_{A_1}$ is the contribution to this state from the diabatic electronic ground state, and σ_{A_1} is the Fermi-contact constant in the electronic ground state.

In the calculation of the A' and B' rotational constants in the prolate limit we use $A'' = 8.002\ cm^{-1}$ and $\overline{B''}(= (B'' + C'')/2) = 0.422\ cm^{-1}$ (the distinct constants being $B'' = 0.4337$ and $C'' = 0.4104$) for the electronic ground state.[8]

One could refine the analysis by treating NO_2 as an asymmetric top. Because in our experiments absolute frequencies could be measured with an accuracy of only $0.02\,cm^{-1}$ and the asymmetry $B-C$ is of the same magnitude, and also because the calculation of A' and $\overline{B'}$ is based on a few transitions at best, we have refrained from doing so. For the first electronically excited state, the asymmetry could be larger, up to about $0.1\,cm^{-1}$ at the equilibrium geometry, where A' is calculated to be $2.84\,cm^{-1}$.[16] In the frequency range studied here, however, the lowest A'-value is found to be about $6.5\,cm^{-1}$, which implies that the asymmetry would be about $0.03\,cm^{-1}$, unless the inertial defect would be unusually large. Thus, the asymmetry would be about equal to that for the ground state.

IV. RESULTS

In this section the results are presented of the measured transitions of the $K_-=1$ stack of the vibronic bands at 13 395.71, 13 352.68, 13 184.57, 12 658.38 and 11 210.65 cm^{-1}. The last value is taken from Ref. 7; the first three band origins are taken from a recent study by Delon and Jost,[22] in which previous laser induced fluorescence (LIF),[23] intracavity laser absorption spectroscopy (ICLAS)[7] and laser induced dispersed fluorescence spectroscopy (LIDFS),[24] are complemented by improved LIF measurements in the region between 11 680 and 13 900 cm^{-1}. The updated values in Ref. 22 may deviate more than $0.1\,cm^{-1}$ from previously cited values.

A. Vibronic band at 13 395 cm^{-1}

The fine structure splitting and hyperfine structure constants obtained from simulating the P(2) and P(3) $K_-=1$ transitions of the $13\,395\,cm^{-1}$ vibronic band are given in Table I.

From the assignments of the P(2) $K_-=1$ transition at $13\,395.92\,cm^{-1}$ and the P(3) $K_-=1$ transition at $13\,395.13\,cm^{-1}$, we determine $C'=0.409\,cm^{-1}$ from the difference between the $N'=1$ and $N'=2$ rotational levels of the $K_-=1$ stack. In this particular case there is no point in using the symmetric top approximation, since only C' enters the energy differences of interest.

The R(0) and P(2) transitions of the $K_-=0$ stack are found at the same transition frequencies as in the ICLAS experiments of Georges *et al.*[7] The A' rotational constant can be calculated from the difference between either of the $K_-=0$ transitions R(0) and P(2), and the P(2) ($K_-=1$) transition, using $C'=0.403$. The two A' values so obtained are equal to 9.87 within $0.01\,cm^{-1}$. $A'=9.87\,cm^{-1}$ is in agreement with the value found from the same transitions, given in Ref. 22, viz. $9.85\,cm^{-1}$. Considerably smaller A' values were found from higher K_- transitions of the $13\,395\,cm^{-1}$ band;[25] Perrin *et al.*[12] found only an average value of $A'=8.74\,cm^{-1}$ from the $K_-=0-4$ transitions.

B. Vibronic band at 13 352 cm^{-1}

The spectra measured for this vibronic band have been reported in a previous paper.[15] Because of the neglect of nondiagonal elements of the spin-rotation coupling, connecting N and $N\pm1$, for $K_-=1$, some features in the Q(1) and Q(2) transitions of the $K_-=1$ stack could not be assigned properly. Taking those nondiagonal elements into account significantly improves the fits of the experimental spectra, but has a minor effect on the results for the Fermi-contact constants and the rotational constants. For completeness, the improved results for the $13\,352\,cm^{-1}$ transition are included in Table I.

From the $K_-=0$ transitions it is found that $\overline{B'}=0.404\,cm^{-1}$, which is in agreement with the value $0.402\,cm^{-1}$ given in Ref. 22. Combining the data for the $K_-=0$ and $K_-=1$ transitions, we find A' values of about $9.5\,cm^{-1}$, which is considerably smaller than $A'=10.6\,cm^{-1}$ given by Delon and Jost.[22] The latter value is, however, considered doubtful by these authors.

C. Vibronic band at 13 184 cm^{-1}

In addition to the R(0) $K_-=0$ transition at $13\,185.42\,cm^{-1}$ (see Ref. 10), we have measured a small part of the energy range in between the R(0) $K_-=0$ transition and the band origin of $13\,184.62\,cm^{-1}$ as determined by Georges *et al.*[7] and reassessed in Ref. 22 as 13 184.57. This is the energy range where the transitions of the $K_-=1$ stack are expected to show up in the absorption spectrum.

Figure 2 shows the measured spectrum between $13\,184.85$ and $13\,185.00\,cm^{-1}$ and the simulation of the experimental spectrum with the P(5), Q(5) and R(5) transitions of the $K_-=1$ stack, respectively, fitted to the most intense lines. Unfortunately, the assignments cannot be made on the basis of absolute frequencies for those transitions, since these are not accurately known from other measurements. The simulations are illustrative of the difficulties that may be encountered in assigning the measured transitions, particularly if transitions between the higher rotational levels are involved, since these all have roughly the same appearance.

The details of the experimental spectrum are best reproduced by the simulated spectrum of the P(5) $K_-=1$ transition, although assignment to the Q(5) $K_-=1$ transition cannot be entirely excluded. Other options, e.g., assigning the transition as P(4) and P(6), give less satisfactory fits of the most intense lines and, moreover, incorrect positions of the central weak hyperfine components around 1500 and 3500 MHz, which are only just visible in the experimental spectrum.

If we assign the spectrum between 1000 and 4200 MHz as P(5) $K_-=1$, it is most obvious to assign the lines around 500 MHz as being part of the P(6) $K_-=1$ transition. However, this leads to an averaged rotational constant $\overline{B'}=0.494\,cm^{-1}$. This is way off the value of $\overline{B'}=0.424\,cm^{-1}$ that is consistent with the position of the R(0) $K_-=0$ band relative to the band origin given by Delon and Jost.[22] Reassigning the $13\,184.99\,cm^{-1}$ transition as Q(5) and identifying the $13\,184.87\,cm^{-1}$ structure with Q(4) or, alternatively, with Q(6), also leads to large discrepancies with the values of $\overline{B'}$ and A' reported by Delon and Jost.[22]

Because we could not scan the spectrum in this region to lower frequencies, we have no clue as to which transition the structure in Fig. 2 around 500 MHz belongs. If we ignore

TABLE I. Fitted fine- and hyperfine structure parameters (in MHz) of transitions belonging to the vibronic band located at 13 395.65, 13 352.68, 13 184.62, 12 658.34 and 11 210.65 cm^{-1}. Errors are two times the standard deviation of the fit.

Band origin (cm^{-1})[a]	Transition	Freq. (cm^{-1})[b]	Exc. level	Fine[c]	σ'	λ'[d]	Rot. const. (cm^{-1})[e]
13 395.71	$K_-=0$[f]			$\overline{\epsilon'}$			
	R(0)	13 396.59	$N'=1$	1086±1	54±1	6±1	
	P(2)	13 394.08	$N'=1$	1086±1	52±1	5±1	
	$K_-=1$			fss			
	P(2)	13 395.92	$N'=1$	7773±1	59±1	−10±1	$C'=0.409$
	P(3)	13 395.13	$N'=2$	−261±2	69±2	−9±8	$A'=9.87$
13 352.68	$K_-=0$[f]			$\overline{\epsilon'}$			
	R(0)	13 353.48	$N'=1$	174±4	121±6	9±2	
	R(2)	13 354.99	$N'=3$	217±1	128±7	3±7	$\overline{B'}=0.404$
	$K_-=1$[g]			fss			
	Q(1)	13 354.18	$N'=1$	6517±1	130±1	−8±3	$A'=9.53$
	Q(2)	13 353.97	$N'=2$	2952±3	123±5	−5±9	$A'=9.40$
	R(1)	13 355.72	$N'=2$	2954±2	123±4	−18±9	$A'=9.45$
13 184.57	$K_-=0$[f]			$\overline{\epsilon'}$			
	R(0)	13 185.42	$N'=1$	530±1	89±1	7±1	
	$K_-=1$[g]			fss			
	P(5)	13 184.99	$N'=4$	−2528±1	103±4	−28±5	$A'=12.62$
12 658.38	$K_-=0$[f]			$\overline{\epsilon'}$			
	R(0)	12 659.28	$N'=1$	778±1	43±1	10±1	
	P(2)	12 656.77	$N'=1$	777±1	42±1	11±1	
	R(0) hot[h]	11 909.59	$N'=1$	777±1	40±1	14±1	
	R(2)	12 661.15	$N'=3$	56±1	61±5	10±4	$\overline{B'}_{13}=0.440$
	P(4)	12 655.24	$N'=3$	56±1	65±4	4±3	
	P(6)	12 653.91	$N'=5$	−20±1	65±1	7±2	$\overline{B'}_{35}=0.442$
	$K_-=1$[g]			fss			
	R(1)	12 659.28	$N'=2$	5453±1	59±2	−13±5	$\overline{B'}=0.432$
	R(3)	12 661.11	$N'=4$		60±9	−12±12	$A'=7.14$
11 210.65	$K_-=0$[f]			$\overline{\epsilon'}$			
	$R_{1/2}(0)$	11 211.50	$N'=1$				
	P(2)	11 208.91	$N'=1$	−1255±1	81±1	−8±1	
	$K_-=1$			fss			
	R(1)	11 211.11	$N'=2$	3208±3	85±5	−12±11	$A'=6.75$
	$K_-=0$ hot band; origin at 11 960.81 cm^{-1}						
	$R_{3/2}(0)$ (0,1,0)	11 211.84	$N'=1$		$\omega_2''=749.66$ [i]		$\overline{B''}=0.423$
	$P_{3/2}(2)$ (0,1,0)	11 209.30	$N'=1$		$\omega_2''=749.68$ cm^{-1} [i]		

[a]Labeling according to Delon and Jost (Ref. 22) and Georges *et al.* (Ref. 7).
[b]Frequencies correspond to transitions between the corresponding rotational levels (without fine- and hyperfine structure splittings). Measured with an accuracy of 0.02 cm^{-1}, as given by the wavemeter manufacturer.
[c]For $K_-=0$, the entry is $\overline{\epsilon}$, for $K_-=1$ it is the fine structure splitting (fss) between the $J=N+1/2$ and $J=N-1/2$ fine structure levels; for a positive splitting the $J=N+1/2$ level is lowest in energy.
[d]For $K_{-1}=1$ stacks, λ' is an effective electron-^{14}N spin dipole-dipole interaction, since τ' is arbitrarily set to zero (see text for explanation).
[e]Rotational constants as calculated from the transition positions of the corresponding row in combination with other transitions in the same vibronic band (see text for further explanation).
[f]See Ref. 10.
[g]For further explanation see text.
[h]The constants of the vibrational ground state of the electronic ground state are used in the simulation.
[i]$\omega_2''=749.6485$ cm^{-1} as determined by Cabana *et al.* (Ref. 26).

this structure and assume that $\overline{B'}=0.423\,cm^{-1}$,[22] the A' rotational constant calculated from the $K_-=0$, R(0) band and the $K_-=1$, P(5) band is 12.62 cm^{-1}, slightly smaller than the value given in Ref. 22, 12.75 cm^{-1}.

D. Vibronic band at 12 658 cm^{-1}

The assignment of the R(0) $K_-=0$ transition is complicated by the overlap with the R(1) $K_-=1$ transition. Our decomposition of the experimental spectrum into the R(0) $K_-=0$ and R(1) $K_-=1$ transitions is supported by measuring this energy region at different temperatures and backing pressures. Further evidence for the correct values of the fit parameters for the $N'=1$ $K_-=0$ rotational level determined via the R(0) $K_-=0$ transition is obtained by measuring the P(2) $K_-=0$ transition and the R(0) $K_-=0$ (0,1,0) hot band.

In addition, we measured transitions to the $N'=3$ [R(2) and P(4) transitions] and $N'=5$ [the P(6) transition] rotational levels of the $K_-=0$ stack.

Figure 3 shows schematically the $K_-=0,1$ transitions

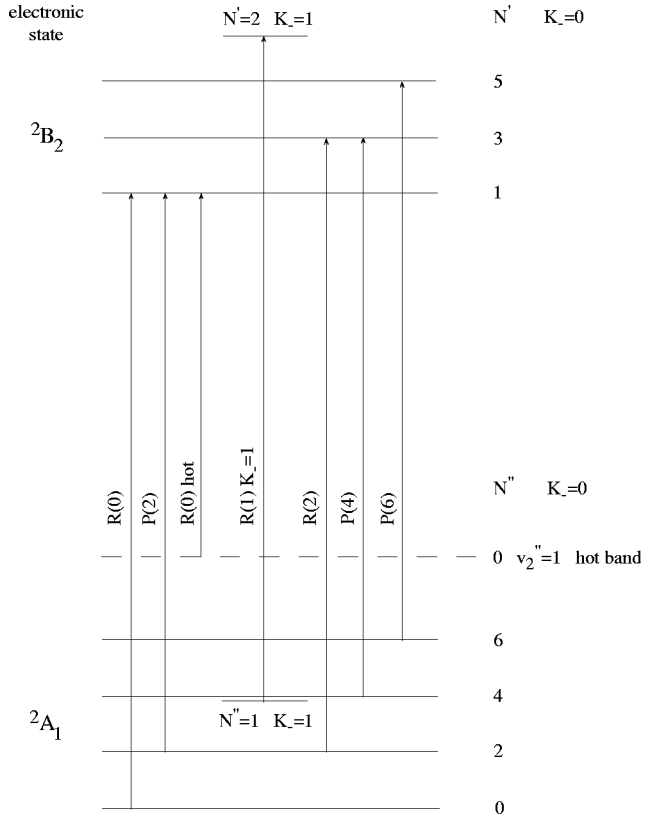

FIG. 3. Schematic overview of the measured transitions and rotational levels involved of the 12 658 vibronic band. The fine- and hyperfine structure splittings are omitted for clarity.

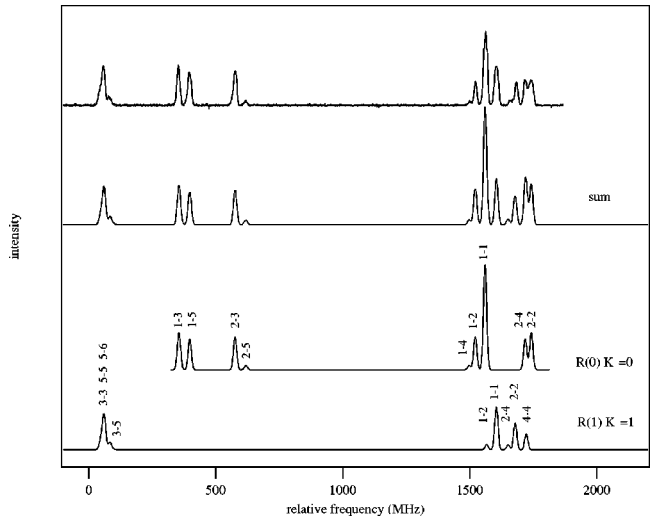

FIG. 4. R(0) $K_-=0$ and R(1) $K_-=1$ transitions at 12 659.28 cm^{-1} of the 12 658 vibronic band. Upper trace: experimental spectrum. Lower traces: simulations. The simulations have been added to obtain a sum spectrum to compare. For an explanation of the line-labeling, see caption, Fig. 2. Note that for the R(0) $K_-=0$ transition, there are only two levels in the ground state, and five in the excited state.

of the vibronic band at 12 658.34 cm^{-1} and the rotational levels involved. Fine- and hyperfine structures are omitted for clarity.

In Fig. 4 we show the experimental spectrum of the energy region around 12 659.28 cm^{-1} where the R(0) $K_-=0$ and R(1) $K_-=1$ transitions overlap. The figure also shows the simulated spectra of the R(0) $K_-=0$ transition, the R(1) $K_-=1$ transition and the sum of both simulated spectra. The sum spectrum is obtained by taking the R(0) $K_-=0$ and R(1) $K_-=1$ spectra with a ratio of 1:0.4 (corresponding to a rotational temperature of 9 K), which is close to the ratio of about 1:0.3 expected for a rotational temperature of 8 K, assumed in Sec. III.

The fine structure constant, Fermi-contact constant and dipole-dipole constant for the R(0) $K_-=0$ transition, as well as the fine structure splitting and hyperfine structure constants obtained from the R(1) $K_-=1$ transition, are listed in Table I.

To verify the assignment of the lines of the R(0) $K_-=0$ transition, we measured the P(2) $K_-=0$ transition and the R(0) $K_-=0$ (0,1,0) hot band. All these transitions have the same $N'=1$ rotational level in common (see Fig. 3). Figure 5 shows the R(0) $K_-=0$ hot band at 11 909.59 cm^{-1}. For the electronic ground state in the simulation of the hot band spectrum we used the fine- and hyperfine constants of the lowest vibrational level of the electronic ground state. The constants obtained from the best fit of these transitions are also listed in Table I and do agree very well with the constants determined for the R(0) $K_-=0$ transition ($\overline{\epsilon'}=778$, $\sigma'=43$, $\lambda'=10$ MHz). From the hot band measurement we determined $\omega_2''=749.69\ cm^{-1}$. This is slightly higher than the value $\omega_2''=749.6485\ cm^{-1}$ given by Cabana *et al.* for the electronic ground state.[26]

Although the R(0), P(2) and R(0) hot band transitions of the $K_-=0$ stack all have the same $N'=1$ rotational level in common, Fig. 4 shows a mismatch in intensity between the experimental and simulated spectra for the $R_{3/2}(0)$ transition around 1600 MHz. A similar, but much smaller mismatch is present in the P(2) spectrum. It is absent, however, in the R(0) hot band spectrum shown in Fig. 5. We shall return to these discrepancies in Sec. V.

The R(2) $K_-=0$ transition connected with the $N'=3$ $K_-=0$ rotational level is shown in Fig. 6.

The Fermi-contact constant obtained via the R(2) and P(4) transitions for the $N'=3$ level of the $K_-=0$ stack is about 63 MHz. For the $N'=5$ level of the $K_-=0$ stack we determined a similar Fermi-contact interaction constant of 65 MHz. The Fermi-contact constant of about 42 MHz, obtained via the R(0), P(2) and R(0) hot band transitions for the $N'=1$ level of the $K_-=0$ stack are similar to each other, but are significantly lower than the Fermi-contact constants of about 64 MHz determined for the other rotational levels.

From the energy differences between the $N'=1$ and $N'=3$ rotational levels of the $K_-=0$ stack we determined $\overline{B'}=0.440\ cm^{-1}$. This is in very good agreement with the averaged rotational constant of $\overline{B'}=0.441\ cm^{-1}$ determined by Georges *et al.*[7] for these rotational levels, and the value given in Ref. 22, $\overline{B'}=0.439\ cm^{-1}$. The energy difference between the $N'=3$ and $N'=5$ rotational levels of the $K_-=0$ stack leads to $\overline{B'}=0.442\ cm^{-1}$, exactly the same as determined by Georges *et al.*

From the small difference between the R(1) $K_-=1$ and

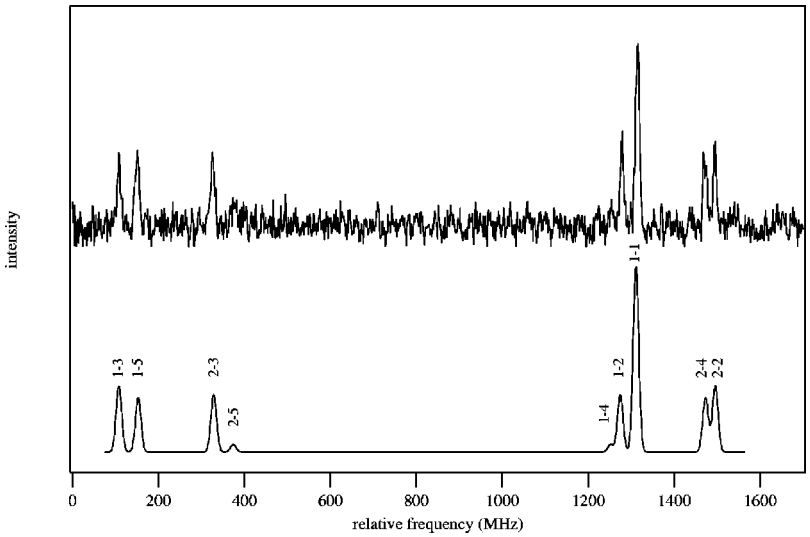

FIG. 5. R(0) $K_-=0$ (0,1,0) hot band at 11 909.59 cm^{-1} of the 11 908 cold vibronic band. Upper trace: experimental spectrum. Lower trace: simulation. For an explanation of the line-labeling, see caption, Figs. 2 and 4.

R(0) $K_-=0$ transitions, and taking $\overline{B}'=0.441\,cm^{-1}$ for the excited state, we determine $A'=7.11\,cm^{-1}$ for the vibronic band at 12 658.38 cm^{-1}. Using these values of $\overline{B}'$ and A', and the band origin, the only transition of the $K_-=1$ stack around 12 661 cm^{-1} is the R(3) $K_-=1$ transition (12 661.24 cm^{-1}). When we assign the lines at 12 661.11 cm^{-1}, see Fig. 6, as the $R_{9/2}(3)$ $K_-=1$ transition, then from the difference of the R(1) and R(3) transitions we determine a $\overline{B}'$ rotational constant of 0.432 cm^{-1} for the $K_-=1$ stack. Using this rotational constant we obtain $A'=7.14\,cm^{-1}$.

The A' value given by Delon and Jost,[22] 8.56 cm^{-1}, is significantly larger. We have found no explanation for this discrepancy.

E. Energy region around 11 210 cm^{-1}

Assignments of the transitions of the vibronic band at 11 210.65 cm^{-1} are complicated by interference from the hot bands of the vibronic band at 11 960.81 cm^{-1}. An additional experimental problem was that the laser would not scan at all frequencies in this energy region, probably because of the abundance of water absorptions in this region.

Via the P(2) $K_-=0$ transition we determined a fine structure constant of -1255 MHz for the $N'=1$ rotational level of the $K_-=0$ stack (see Ref. 10 and Table I). Combining this fine structure constant with the measured $R_{1/2}(0)$ $K_-=0$ transition at 11 211.50 cm^{-1}, the $R_{3/2}(0)$ $K_-=0$ transition is expected at 11 211.43 cm^{-1}. Unfortunately, we could not scan this part of the absorption spectrum because of experimental problems. However, we measured a quite weak $R_{3/2}(0)$ $K_-=0$ transition at 11 211.84 cm^{-1}, which does not belong to the 11 210 vibronic band. We were able to assign this transition as the $R_{3/2}(0)$ $K_-=0$ (0,1,0) hot band of the 11 960 vibronic band. One doublet of this hot band was expected to occur at 11 211.89 cm^{-1} by Jost.[25] The corresponding $R_{3/2}(0)$ $K_-=0$ cold band of the 11 960 cold vibronic band is found at 11 961.50 cm^{-1}.[10] From the difference between the cold band and the corresponding hot band we determine $\omega_2''=749.66\,cm^{-1}$, which is very close to the value of $\omega_2''=749.6485\,cm^{-1}$ found by Cabana *et al.*[26]

The $P_{3/2}(2)$ $K_-=0$ (0,1,0) hot band of the cold vibronic band at 11 961 cm^{-1} is measured at 11 209.30 cm^{-1} (expected at 11 209.36 cm^{-1} by Jost[25]). The difference between the hot band and cold band leads to $\omega_2''=749.68\,cm^{-1}$. From the $R_{3/2}(0)$ $K_-=0$ and $P_{3/2}(2)$ $K_-=0$ (0,1,0) hot bands we determine $\overline{B}''=0.423\,cm^{-1}$ for the vibrational level of the electronic ground state with one quantum in the symmetric bending mode.

The fine structure splitting and hyperfine structure constants obtained from the best fit of the R(1) $K_-=1$ transition at 11 211.11 cm^{-1} are listed in Table I. From the measured $R_{1/2}(0)$ $K_-=0$ transition at 11 211.50 cm^{-1} and taking $\overline{B}'=0.440\,cm^{-1}$,[7] we determine $A'=6.75\,cm^{-1}$ from the R(1) $K_-=1$ transition at 11 211.11 cm^{-1}.

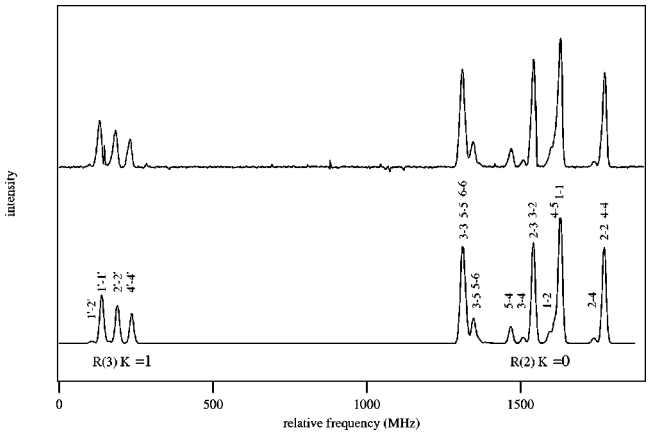

FIG. 6. R(2) $K_-=0$ transition at 12 661.15 cm^{-1} of the 12 658 vibronic band. The lines around 200 MHz, however, are most likely to be assigned to a fine structure component of the R(3) $K_-=1$ transition, as the simulated spectrum (below) shows. Upper trace: experimental spectrum. Lower trace: R(2) $K_-=0$ and R(3) $K_-=1$ simulations. For an explanation of the line-labeling, see caption, Fig. 2. The labels for the $K_-=1$ transition lines are distinguished from those of the R(2) $K_-=0$ transition by primes.

TABLE II. Determined Fermi-contact constant, σ', A' rotational constant and contributions of the electronic ground state and first electronically excited state for the measured vibronic bands. The Fermi-contact constant of the ground vibronic state is 147.26 MHz (Ref. 8). Also included are A' values given in Ref. 22. Entries in the last column are calculated, hypothetical, A_{A_1} values for the vibrational level(s) of the electronic ground state, participating in the excited hybrid state.

Vibr. band	σ' (MHz)	A' (cm^{-1})	A' (cm^{-1})[a]	($\tilde{X}\,^2A_1$ %)	($\tilde{A}\,^2B_2$ %)	A_{A_1} (cm^{-1})
13 395	P(2): 59	9.87	9.85	40	60	20.6
	P(3): 69			47	53	17.9
13 352[b]	Q(1): 130	9.53		88	12	10.5
	Q(2): 123	9.40	10.6[c]	84	16	10.7
	R(1): 123	9.45		84	16	10.7
13 184	P(5): 103	12.62	12.75	70	30	16.9
12 658	R(1): 59	7.14	8.65	40	60	13.8
	R(3): 60			41	59	13.5
11 210	R(1): 85	6.75		58	42	9.2

[a]From Ref. 22.
[b]See Ref. 15.
[c]Considered doubtful (Ref. 22).

V. DISCUSSION

The experimental bolometric spectra are fitted to a fine structure splitting, a Fermi-contact interaction constant, σ', and a dipolar electron spin-nuclear spin interaction constant, λ'. Similar to the $K_-=0$ stack,[10] the transitions of the $K_-=1$ stack are simulated under the assumption that the effective Hamiltonian model is valid. The very good agreement between the experimental and calculated relative intensities for four of these transitions is an indication of the absence of appreciable rovibronic interactions implicitly excluded in the effective Hamiltonian model. If rovibronic interactions were completely absent, one could expect that the Fermi-constants obtained for different rotational states in a given vibronic state would be equal. The σ' values found for different rotational levels in each of the vibronic bands at 11 210, 13 352, and 13 395 cm^{-1} have comparable values (see Tables I and II), indicating that rovibronic interactions are weak. Also for the $N'=2$ to 5 rotational levels of the 12 658 cm^{-1} vibronic band, σ' values between 59 and 65 MHz are found. As mentioned above, the $N'=1$ rotational sublevel of this band behaves differently (*vide infra*). For the 13 184 cm^{-1} band, the σ' values for the $N'=1$ and $N'=4$ levels have still comparable values, though the difference is somewhat larger than in the foregoing examples.

In general, such differences may be attributed to small rovibronic interactions. As explained previously by Delon *et al.*,[27] rovibronic interactions may couple, for instance, $N=1$, $K_-=0$ B_2 vibronic states with $N=1$, $K_-=1$ or $N=2$, $K_-=1$ A_2 vibronic states. If the coupling is strong enough, transitions to otherwise dark states become possible, resulting in ''extra lines.'' [27] If the rovibronic interactions are weak, they may, in principle, still lead to noticeable changes in the *effective* hyperfine coupling constant (and generally larger changes in the fine structure splitting), whereas the intensity changes of the (hyper)fine structure remain small. The effective constants are obtained from a fit under the assumption that rovibronic couplings are absent, and thus are related to the level shifts caused by the rovibronic interaction. The level shifts determine the degree of mixing, whereas the intensities depend on the squares of the mixing coefficients.

We have also considered the possibility of a local rovibronic coupling to explain the difference between the σ' value for the $N'=1$ level and the σ' values of the $N'=2-5$ levels of the 12 658 cm^{-1} vibronic band. Moreover, this should also explain the intensity mismatch between the $R_{3/2}(0)$ $K_-=0$ and the $R_{1/2}(0)$ $K_-=0$ lines, Fig. 4, mentioned above. Specifically, rovibronic coupling with an $N=2$, $K_-=1$ state of another vibronic band would only affect the $J=3/2$ levels, i.e., decrease the intensity of the transitions to those levels, and not to the $J=1/2$ levels, which is just what is observed for the R(0) and P(2) spectra. If there were multiple rovibronic couplings, one would also expect deviations from the calculated intensities for the hyperfine components of the lines, as is observed for higher-lying vibronic states (see, e.g., Ref. 28; see also a recent study[29] in which transient grating spectroscopy is used to resolve hyperfine structures in the 20 500 cm^{-1} region). This is not the case here, which indicates that, if rovibronic interaction plays a role, only a single coupling is involved. The coupling should be strong enough in order to decrease the intensities of the $J=3/2$ lines appreciably. Apart from affecting the line intensities, the rovibronic interaction could also explain the much larger fine structure splitting compared with those found from the R(2), P(4) and P(6) transitions to $N'=3$ and $N'=5$ of the $K_-=0$ stack (see Table I). In addition, the difference between the (effective) Fermi constants found for these rotational states would be accounted for.

This explanation is, however, not quite satisfactory as far as the line intensities are concerned. If the mismatch of line intensities in the R(0) $K_-=0$ spectrum is to be explained by a rovibronic coupling, this cannot at the same time explain why the discrepancy is much smaller in the P(2) spectrum and even almost absent in the R(0) hot band spectrum. We have not yet found an explanation for this puzzling result.

At this point it is of interest to mention an observation by Delon and Jost[22] (see also Ref. 30), namely that the next neighbor spacing distribution changes rather abruptly from

the fourth polyad (around 11 960 cm^{-1}) to the fifth polyad. Since the last polyad is around 12 650 cm^{-1}, this observation may have a bearing on the interpretation of our results for the 12 658 cm^{-1} band described above.

In Table II, the Fermi-contact constants, σ', and A' values are listed as determined from the $K_-=1$ stack transitions. Furthermore, the relative contributions of the electronic ground state and first electronically excited state are given as determined by the Fermi-contact constants.

The Fermi-contact constant obtained via the $K_-=1$ stack transitions is in most cases similar to the Fermi-contact constant obtained via the $K_-=0$ stack of the same vibronic band.

The last column of Table II lists the A_{A_1} rotational constant obtained for the high vibrational level(s) of the electronic ground state as calculated by $[A'=q^n_{A_1}A_{A_1}(E_n)+q^n_{B_2}A_{B_2}(E_n)]$. We used $A_{B_2}=2.72\ cm^{-1}$ for the first diabatic electronically excited state and the measured A'-value for the hybrid excited state.

The significant Fermi-contact constant for the 11 210 vibronic band shows the strong vibronic coupling of the electronic ground state and first electronically excited state as low as 11 210 cm^{-1}. The large contribution of the electronic ground state in the hybrid excited states is confirmed by the A' rotational constants deduced from the $K_-=1$ stack measurements.

The 13 395 vibronic band, the 12 658 vibronic band and the 11 210 vibronic band all have roughly half the character of each of the electronic ground state and first electronically excited state. The contribution of the first electronically excited state is assigned to originate mainly from vibrational levels with quanta in the bending mode. According to calculations by Leonardi and Petrongolo,[31] the 13 395, 12 658 and 11 210 vibronic bands are associated with the (0,5,0), (0,4,0) and (0,2,0) vibrational levels of the first electronically excited state, respectively.

Vibrational levels of the first electronically excited state will mainly couple to nearby vibrational levels of the electronic ground state, so stepping down the bending vibrational ladder in the first electronically excited state, we expect to step down in the vibrational ladder of the electronic ground state as well, for which levels the molecule has a decreasing A_{A_1} rotational constant. For the vibronic bands at 13 395, 12 658 and 11 210 cm^{-1} one can see that the A_{A_1} rotational constant associated with the coupled high vibrational level(s) of the electronic ground state, indeed decreases with decreasing vibronic band energy.

Calculations by Hallin and Merer[11] of the A_{A_1} rotational constant for high vibrational levels of the electronic ground state, show that for a given vibrational energy the A_{A_1} rotational constant is higher for vibrational levels with a relatively large number of quanta in the bending mode. The 13 395 vibronic band is illustrative of such a type of behavior. The $^2B_2$-electronic character of this vibronic band is found to be mainly associated with the (0,5,0) vibrational level of the first electronically excited state. The large value of the A_{A_1} rotational constant suggests that the $^2A_1$-electronic character is also associated with a vibrational level with relatively many quanta in the symmetric bending mode. The 13 352 vibronic band corresponds to a similar energy as well as a similar A' value compared to the 13 395 vibronic band. The electronic character of the 13 352 vibronic band, however, is mainly $^2A_1$ (see Ref. 10 and Table II). Moreover, the relatively small A_{A_1} value indicates that the vibrational character is also completely different from that of the 13 395 vibronic band.

VI. SUMMARY

In the present paper we analyzed transitions of the $K_-=1$ stacks of five different vibronic bands, one of which was studied previously.[15] In the analyses, rovibronic interactions are assumed to be absent. This assumption is corroborated by the excellent agreement of the calculated with the measured line intensities, and the similarity of the Fermi-contact interaction constants for different rotational sublevels of the same vibronic band. Then the Fermi-contact interaction constant may be used as a quantitative measure of the electronic ground state character of the vibronic states studied.

The mismatches found in the intensities of the fine structure components of different transitions to the $N'=1$ level of the 12 658 cm^{-1} band, may partly be explained by a rovibronic interaction with a single other vibronic state. Such an interaction could also explain the differences in σ' values between the $N'=1$ rotational substate on the one hand, and the $N'=2-5$ substates on the other, as well as the difference in the hyperfine splittings between the $N'=1$ and $N'=3$ and 5 levels. If the interaction is real, its identification could help in identifying the vibronic state involved. The intensity mismatch between the two hyperfine components is, however, not the same for different transitions from the ground state to the $N'=1$ level. We have not yet found a satisfactory explanation for this behavior.

In contrast to the transitions of the $K_-=0$ stacks, transitions of the $K_-=1$ stacks also provide values of the A' rotational constants in the excited vibronic state. A clear correlation is found between the Fermi-constants, σ', and the A' constants, as could be expected, since both depend on the relative contribution of the constituent electronic states in the vibronic state. In addition, the A' constant also depends on the nature of the vibrational states that contribute to the vibronic state.

Therefore, measuring both σ' and A' values and combining these with calculations of the vibrational decomposition and assignments, such as carried out by Leonardi and Petrongolo,[31] and more recently also by Salzgeber *et al.*,[32] is a valuable tool in analyzing the nature of vibronic states. Such a combination of experiment and theory is promising for a reliable electronic and vibrational characterization of the vibronic levels in NO_2. Starting at the conical intersection it might provide a sound basis for attempts to characterize higher-lying vibronic states up into the chaotically behaving region.

ACKNOWLEDGMENTS

The authors thank Professor R. Jost for clarifying discussions and for making results available prior to publication. Part of the work of M.H.M.J. was made possible by a fellowship of the Royal Dutch Academy of Arts and Sciences (KNAW). The Dutch Organization for Scientific Research, NWO, is acknowledged for support through FOM and CW.

[1] D. K. Hsu, D. L. Monts, and R. N. Zare, *Spectral Atlas of Nitrogen Dioxide* 5530 to 6380 Å (Academic, New York, 1978).
[2] R. E. Smalley, L. Wharton, and D. H. Levy, J. Chem. Phys. **63**, 4977 (1975).
[3] A. C. van Daele, C. Hermans, P. C. Simon, M. Carleer, R. Colin, S. Fally, M. F. Mérienne, A. Jenouvrier, and B. Coquart, J. Quant. Spectrosc. Radiat. Transf. **59**, 171 (1998).
[4] H. Köppel, W. Domcke, and L. S. Cederbaum, in *Advances in Chemical Physics*, edited by I. Prigogine and S. A. Rice (Wiley, New York, 1984), Vol. 57, p. 59.
[5] G. Hirsch, R. J. Buenker, and C. Petrongolo, Mol. Phys. **73**, 1085 (1991).
[6] G. Persch, E. Mehdizadeh, Th. Zimmermann, W. Demtröder, H. Köppel, and L. S. Cederbaum, Ber. Bunsenges. Phys. Chem. **92**, 312 (1988).
[7] R. Georges, A. Delon, F. Bylicki, R. Jost, A. Campargue, A. Charvat, M. Chenevier, and F. Stoeckel, Chem. Phys. **190**, 207 (1995).
[8] W. C. Bowman and F. C. De Lucia, J. Chem. Phys. **77**, 92 (1982).
[9] H. J. Vedder, G. Persch, and H.-J. Foth, Chem. Phys. Lett. **114**, 125 (1985).
[10] C. A. Biesheuvel, J. Bulthuis, M. H. M. Janssen, J. G. Snijders, and S. Stolte, J. Chem. Phys. **109**, 9701 (1998).
[11] K-E. J. Hallin and A. J. Merer, Can. J. Phys. **55**, 2101 (1977).
[12] A. Perrin, C. Camy-Peyret, J. M. Flaud, and P. Luc, J. Mol. Spectrosc. **88**, 237 (1981).
[13] J. C. D. Brand, W. M. Chan, and J. L. Hardwick, J. Mol. Spectrosc. **56**, 309 (1975).
[14] J. C. D. Brand, K. J. Cross, and A. R. Hoy, Can. J. Phys. **57**, 428 (1979).
[15] C. A. Biesheuvel, D. H. A. ter Steege, J. Bulthuis, M. H. M. Janssen, J. G. Snijders, and S. Stolte, Chem. Phys. Lett. **269**, 515 (1997).
[16] G. D. Gillispie and A. U. Khan, J. Chem. Phys. **65**, 1624 (1976).
[17] For the corresponding spectra of the $K_{-}=0$ stack see C. A. Biesheuvel, J. Bulthuis, M. H. M. Janssen, J. G. Snijders, and S. Stolte, J. Chem. Phys. **109**, 9701 (1998).
[18] R. N. Zare, *Angular Momentum* (Wiley, New York, 1988).
[19] W. H. Press, B. P. Flannery, S. A. Teukolsky, and W. T. Vetterling, *Numerical Recipes* (Cambridge University Press, Cambridge, 1989).
[20] C. C. Lin, Phys. Rev. **116**, 903 (1959).
[21] J. M. Brown and T. J. Sears, J. Mol. Spectrosc. **75**, 111 (1979).
[22] A. Delon and R. Jost, J. Chem. Phys. **110**, 4300 (1999).
[23] R. Georges, A. Delon, and R. Jost, J. Chem. Phys. **103**, 1732 (1995).
[24] B. Kirmse, A. Delon, and R. Jost, J. Chem. Phys. **108**, 6638 (1998).
[25] R. Jost, private communication.
[26] A. Cabana, M. Laurin, W. J. Lafferty, and R. L. Sams, Can. J. Phys. **53**, 1902 (1975).
[27] A. Delon, R. Georges, and R. Jost, J. Chem. Phys. **103**, 7740 (1995).
[28] G. Persch, H. J. Vedder, and W. Demtröder, J. Mol. Spectrosc. **123**, 356 (1987).
[29] Y. Tang, J. P. Schmidt, and S. A. Reid, J. Chem. Phys. **110**, 5734 (1999).
[30] J. Orphal, S. Dreher, S. Voigt, J. P. Burrows, R. Jost, and A. Delon, J. Chem. Phys. **109**, 10217 (1998).
[31] E. Leonardi and C. Petrongolo, J. Chem. Phys. **106**, 10066 (1997).
[32] R. F. Salzgeber, V. A. Mandelshtam, Ch. Schlier, and H. S. Taylor, J. Chem. Phys. **110**, 3756 (1999).